Polymersomes Hot Paper

Deutsche Ausgabe: DOI: 10.1002/ange.201412406
Internationale Ausgabe: DOI: 10.1002/anie.201412406

Polymersomes Prepared from Thermoresponsive Fluorescent Protein–Polymer Bioconjugates: Capture of and Report on Drug and Protein Payloads**

*Chin Ken Wong, Alistair J. Laos, Alexander H. Soeriyadi, Jörg Wiedenmann, Paul M. G. Curmi, J. Justin Gooding, Christopher P. Marquis, Martina H. Stenzel, and Pall Thordarson**

Abstract: *Polymersomes provide a good platform for targeted drug delivery and the creation of complex (bio)catalytically active systems for research in synthetic biology. To realize these applications requires both spatial control over the encapsulation components in these polymersomes and a means to report where the components are in the polymersomes. To address these twin challenges, we synthesized the protein–polymer bioconjugate PNIPAM-b-amilFP497 composed of thermoresponsive poly(N-isopropylacrylamide) (PNIPAM) and a green-fluorescent protein variant (amilFP497). Above 37°C, this bioconjugate forms polymersomes that can (co-)encapsulate the fluorescent drug doxorubicin and the fluorescent light-harvesting protein phycoerythrin 545 (PE545). Using fluorescence lifetime imaging microscopy and Förster resonance energy transfer (FLIM-FRET), we can distinguish the co-encapsulated PE545 protein inside the polymersome membrane while doxorubicin is found both in the polymersome core and membrane.*

[*] C. K. Wong, A. J. Laos, Dr. A. H. Soeriyadi, Prof. J. J. Gooding, Assoc. Prof. P. Thordarson
School of Chemistry, The Australian Centre for NanoMedicine and the ARC Centre of Excellence in Convergent Bio-Nano Science and Technology, The University of New South Wales
Sydney, 2052, NSW (Australia)
E-mail: p.thordarson@unsw.edu.au

Prof. J. Wiedenmann
Coral Reef Laboratory/Institute for Life Science (IfLS)
University of Southampton, Southampton, SO14 3ZH/SO17 1BJ (UK)

Prof. P. M. G. Curmi
School of Physics, The University of New South Wales
Sydney, 2052, NSW (Australia)

Dr. C. P. Marquis
School of Biotechnology and Biomolecular Sciences
The University of New South Wales, Sydney NSW 2052 (Australia)

C. K. Wong, Prof. M. H. Stenzel
School of Chemistry, Centre for Advanced Macromolecular Design
The University of New South Wales, Sydney, 2052, NSW (Australia)

[**] This work was supported by the Australian Research Council (ARC) centre of excellence grant (grant number CE140100036) to P.T. and J.J.G., an ARC Future Fellowship (FT120100101) to P.T., support from the Faculty of Science UNSW to C.P.M. and P.T. and the Australian Government for PhD scholarship to A.J.L.. C.K.W. is grateful for an ARC and UNSW PhD scholarship.

Supporting information for this article is available on the WWW under http://dx.doi.org/10.1002/anie.201412406.

Inspired by nature, where compartmentalization of biological components is all pervasive, we are interested in developing a platform technology of self-assembled multifunctional compartments with applications in areas ranging from nanomedicine[1–4] to synthetic biology.[1,2,5–8] Vesicles and polymersomes that either contain entrapped biomolecules[9–11] or are made from protein–polymer biohybrids[12–14] are the archetypical example of such multifunctional systems. Due to their enhanced stability when compared to liposomes, polymersomes are particularly attractive for applications such as targeted drug delivery.[2,4,15–16] For similar reasons they also provide a good platform for compartmentalizing multienzyme cascades[10] and other sophisticated systems related to synthetic biology.[17,18] There are, however, a number of challenges with polymersomes. These challenges include: 1) the formation and morphology is not easily controlled, making methods to initiate the formation of well-defined polymersomes highly valuable, 2) designing a generic polymersome system that can encapsulate a payload ranging from drugs to proteins at precise locations in the polymersomes, and 3) a means of monitoring the location and status of the payload of interest within the polymersome.

Herein, we report the preparation of well-defined, multifunctional, biohybrid polymersomes that responds to all these challenges. The polymersomes are formed by the self-assembly of fluorescent protein–thermoresponsive polymer bioconjugates (Scheme 1). The design of the polymer component is crucial to the final polymersome function and the versatility of the system. A narrow polydispersity of the polymer–protein conjugate ensures that well-defined low-polydispersed polymersomes are formed. The thermoresponsive polymer component, ideally around 37 °C, corresponding to human body temperature, provides a means to form and dissociate the polymersomes so drugs and proteins can be loaded and released from the polymersomes by simply changing the temperature. Further, the fluorescence property of the protein component allows a combination of fluorescence lifetime imaging microscopy (FLIM) and Förster resonance energy transfer (FRET; FLIM-FRET[19–21]) which precisely reveals the location of the encapsulate within the polymersome.

To incorporate fluorescence in the polymersomes, we selected a green-fluorescent protein derived from the reef coral species *Acropora millepora* (amilFP497).[22] The 27.3 kDa protein is characterized by an absorption and emission maxima of 477 and 497 nm, respectively. The protein contains a free cysteine residue at position 119 for

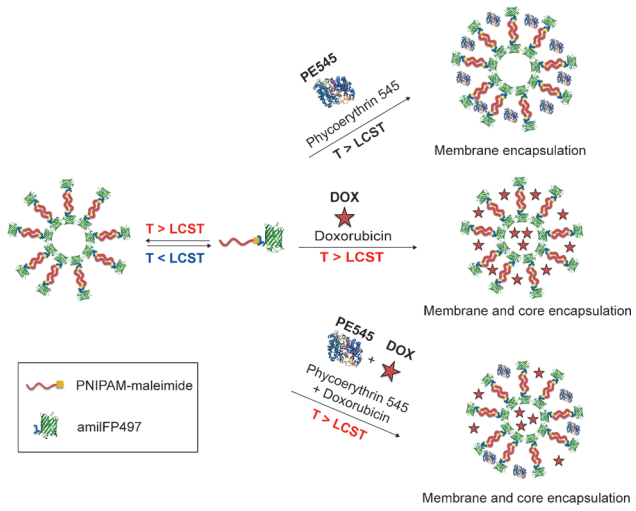

Scheme 1. Polymersomes formed by self-assembly of PNIPAM-*b*-amFP497 bioconjugates upon heating above the lower critical solution temperature (LCST). The biohybrid polymersomes were found to be capable of encapsulating a payload such as the red-fluorescent light-harvesting protein (PE545) and a small organic drug molecule (doxorubicin). However, encapsulation within the polymersomes appeared to be size-dependent. The PE545 protein was found to be encapsulated primarily within the membrane of the polymersomes whereas doxorubicin was found to be encapsulated both within the membrane and in the aqueous core of the polymersomes. The polymersomes are depicted as unilamellar bilayer with the hydrophilic (positively charged at pH 7) amilFP497 acting as the polar head-group of the block copolymer. Note, however, that a multilayer membrane structure cannot fully be ruled out.

site-selective bioconjugation with a maleimide-terminated polymer.

In this study, we used poly(*N*-isopropylacrylamide) (PNIPAM), a thermoresponsive polymer which undergoes transitions from being hydrophilic to hydrophobic upon heating above a lower critical solution temperature (LCST).[23] Olsen and co-workers have previously shown that PNIPAM-fluorescent proteins are a powerful tool to study protein–polymer block copolymer assembly.[24,25] We envisaged that the use of this thermoresponsive polymer would confer temperature responsiveness to both the bioconjugate and its resulting self-assembled structure.

The polymer with an estimated calculated molecular weight ($M_{n,NMR}$) of 9420 g mol^{-1} and a degree of polymerization (DP_n) of 80, was synthesized by reversible addition–fragmentation chain transfer (RAFT) polymerization and subsequently modified to bear a maleimide functional group which readily reacts with a cysteine residue as shown in the Supporting Information (Figures S1–S5).[26] The end-functional maleimide group was identified by the presence of a characteristic maleimide signal observed at $\delta = 6.7$ ppm in the ^{1}H NMR spectrum of the polymer (see Figure S1). The dispersity index of the modified polymer was determined to be 1.10 by gel permeation chromatography in *N*,*N*-dimethylacetamide.

Conjugation of the maleimide-modified polymer to amilFP497 was performed in 20 mM sodium phosphate buffer (pH 7.4) containing 20 mM ethylenediaminetetracetic acid (EDTA). Successful bioconjugation was validated by matrix-assisted laser desorption/ionization time-of-flight (MALDI-TOF) mass spectrometry and fast protein liquid chromatography (FPLC).

The (MALDI-TOF) mass spectrometry (Figure 1 A and Figure S6) analysis shows a broad peak corresponding to the bioconjugate at about 38500 g mol^{-1} (Figure 1 A). The intensity of the bioconjugate peak in the mass spectrum cannot be used for quantitative analysis as the ionization of protein–polymer bioconjugates has been known to be more difficult than native proteins.[27] Interestingly, a small peak observed at 46000 g mol^{-1} (Figure 1 A, inset) suggests that there may be two PNIPAM chains attached onto the protein. This could also explain why there is a small shoulder at the start of the size-exclusion chromatograph in Figure 1 B. Since the polymer was used in excess to react with the protein, we propose that some of the maleimide-bearing polymers may have reacted with primary amines of surface lysine residues or even additional cysteine residues buried inside the protein.

Further evidence of successful bioconjugation was observed during the purification of the crude bioconjugate

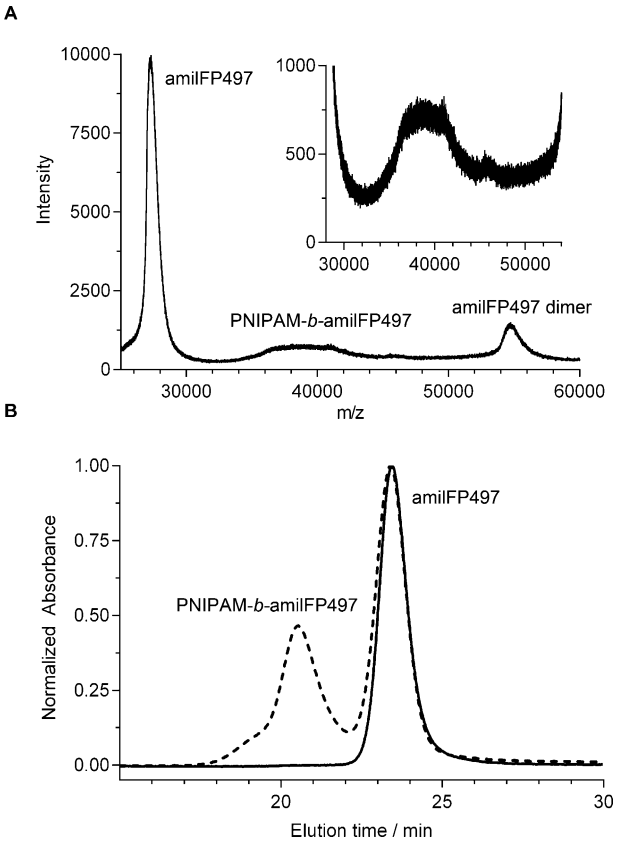

Figure 1. A) MALDI-TOF mass spectrum of a desalted crude mixture of maleimide-terminated PNIPAM and amilFP497 after reaction for 17 h. The inset shows the enlarged region where the PNIPAM-*b*-amilFP497 peak was observed. B) Overlay of size-exclusion chromatography (SEC) traces showing peaks corresponding to PNIPAM-*b*-amFP497 (dotted line) and amilFP497 (solid line). The SEC column was eluted with phosphate buffered saline (pH 7.4) and the detector was set to monitor the absorbance at 477 nm.

reaction mixture by fast protein liquid chromatography (FPLC). The FPLC size-exclusion chromatography (SEC) trace of the crude bioconjugate mixture showed two peaks corresponding to the elution of unreacted amFP497 and the higher molecular weight PNIPAM-*b*-amilFP497, as shown in Figure 1 B. The conjugation efficiency was determined to be 40 % by comparing the integrations of the two peak areas.

Minimal changes in the amilFP497 absorption and emission spectra upon bioconjugation with PNIPAM (see Figure S7) indicated that the amilFP497 proteins remains folded and are still in their native state after bioconjugation. To further investigate the thermoresponsive behavior of PNIPAM-*b*-amilFP497, a cloud point profile of normalized absorbance against temperature (see Figure S9) was plotted and the lower critical-solution temperature (LCST) was determined to be 36.5 ± 0.5 °C—a transition ideally correlated with the normal human body temperature.

The presence of the fluorescent protein in the bioconjugate allows the investigation of PNIPAM-*b*-amilFP497 self-assembly using confocal microscopy. No distinct morphology was observed in a solution of PNIPAM-*b*-amilFP497 bioconjugates analyzed at room temperature (see Figure S10). However, upon heating to 37 °C, circular particles that resemble polymersomes were observed, as shown in Figure 2 A. The average external diameter and average membrane thickness of the polymersomes were found to be 2085 ± 297 and 290 ± 36 nm, respectively (histograms in Figures S12 and S13). The measured thickness suggests these vesicles might be multilamellar, however, given the resolution limit of confocal microscopy is in the order of 250 nm, this value cannot be relied upon. The hollow cores present within individual polymersomes are revealed from a 3D representation obtained from a collection of 79 images across different z heights (Figure 2 B). Attempts to resize the polymersomes by sonication were only moderately successful—the average diameter increased to 2230 ± 354 nm (Figures S14 and S15), however the polydispersity also appeared to increase with signs of protein degradation in the images.

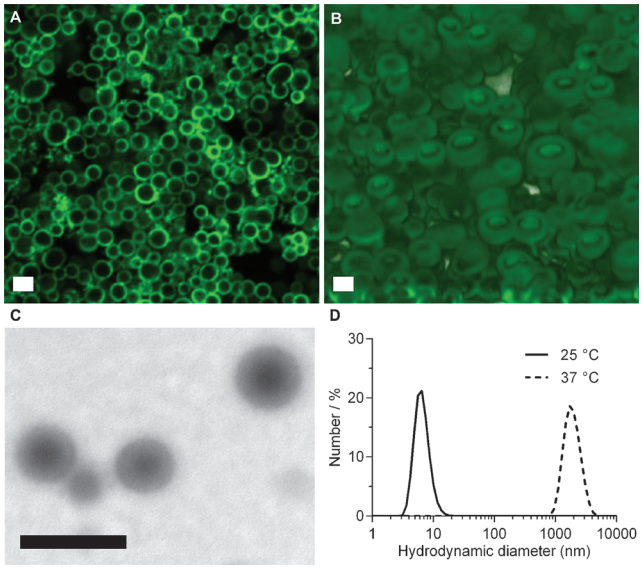

Figure 2. A) Confocal laser scanning microscopy (CLSM) image and B) lateral view of a z-stack image of polymersomes formed from PNIPAM-*b*-amilFP497 bioconjugates in 20 mM sodium phosphate and 20 mM EDTA buffer (pH 7.4) at 37 °C. The scale bar represents 2 μm. C) Transmission electron microscopy (TEM) image (unstained) of PNIPAM-*b*-amilFP497 incubated at 37 °C prior to analysis. D) Particle size distribution from dynamic light scattering (DLS) of PNIPAM-*b*-amilFP497 in 20 mM sodium phosphate, 20 mM EDTA buffer (pH 7.4) at 25 and 37 °C. The scale bar represents 2 μm.

Further evidence of the polymersome morphology was obtained by transmission electron microscopy (TEM). The TEM images showed spherical particles with an average external diameter of 1292 ± 184 nm (Figure S16), dark outlines, and distinct inner contrasts (Figure 2 C), which is consistent with polymersome formation.[28,29] The polymersomes observed by TEM appeared to have a smaller average external diameter to those observed by CLSM but this difference can easily be attributed to the drying effect during the TEM specimen preparation. To further support our claims regarding the size of these polymersomes, the average hydrodynamic diameter (d_h) of the polymersomes was studied using dynamic light scattering (DLS) (Figure 2 D). At 25 °C, the PNIPAM-*b*-amilFP497 bioconjugates had a d_h of 22 ± 0.54 nm. When heated to 37 °C, particles with d_h of 2005 ± 211 nm and polydispersity index (PDI) of 0.21 were observed. The d_h of the polymersomes is in good agreement with the polymersome sizes observed under CLSM.

To explore the potential of using PNIPAM-*b*-amilFP497 and related polymersomes as nanocarriers, encapsulation experiments involving acceptor fluorophores were performed. Successful encapsulation was determined by measuring FRET from amilFP497 (located in the membrane PNIPAM-*b*-amilFP497 polymersomes) to the encapsulated fluorophores, using fluorescence lifetime imaging microscopy (FLIM). We identified two suitable spectrally overlapping fluorophores for the experiment; namely the light-harvesting phycoerythrin 545 (PE545)[30,31] and a common anti-cancer drug: doxorubicin hydrochloride (DOX). Both the excitation spectra of PE545 and DOX overlap with emission spectra for amilFP497 (see Figures S17 and S18 for spectral overlap).

Samples containing a mixture of the PNIPAM-*b*-amilFP497 and the FRET acceptors were initially imaged at 25 °C showing little to no energy transfer, and subsequently heated to 40 °C to encapsulate an acceptor facilitating energy transfer as the PNIPAM-*b*-amilFP497 donor came within Förster distance of the acceptor, leading to a quenched lifetime of the donor. Two detectors were used to investigate the donor–acceptor system, one for the lifetime of the PNIPAM-*b*-amilFP497 donor (485/32 nm—32 nm bandpass filter centered at 485 nm) corresponding to the amilFP497 emission and another to measure the lifetime of the acceptors (617/73 nm—73 nm bandpass filter centered at 617 nm) focused on the acceptor emission spectra, with the lifetime data plotted on a false color scale as shown in Figure 3. The fluorescence lifetime data were analyzed using both exponential tail fitting for the determination of lifetimes, and by phasor analysis[32] to investigate the location of the lifetimes of interest (see the Supporting Information for full analysis).

Initially, PNIPAM-*b*-amilFP497 was imaged as a control (Figure S19, Table S1), and we found that the green fluores-

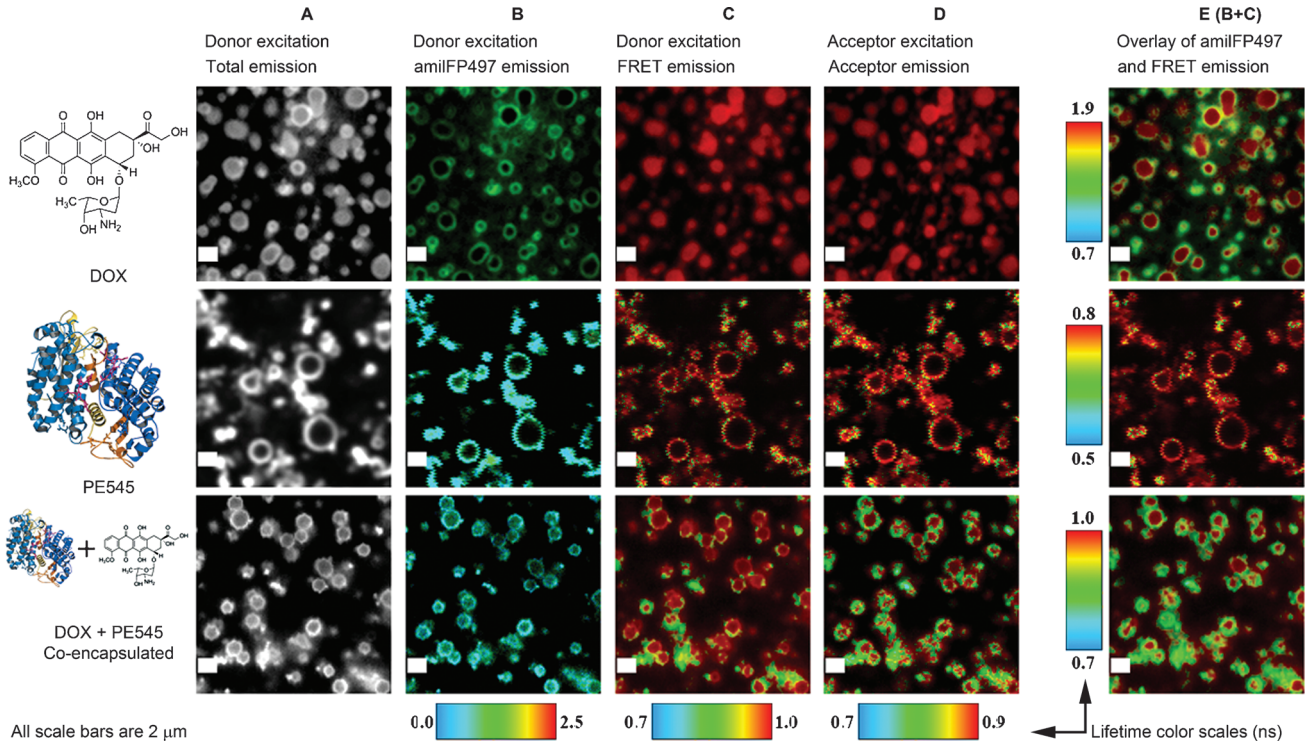

Figure 3. Fluorescence lifetime imaging microscopy (FLIM) images of PNIPAM-*b*-amilFP497 polymersomes formed at 40 °C with encapsulated doxorubicin (DOX, top row), phycoerythrin 545 (PE545, middle row), and a co-encapsulated mixture of DOX and PE545 (bottom row). Images in columns A, B, C, and the overlay in E (B + C) were obtained using 405 nm excitation whereas images in column D were obtained using 532 nm excitation. The relevant lifetime color scales (in nanoseconds) are shown under columns B–D while for the images in column E the colorscale is shown to the left of these images. A) Gray-scale fluorescence image of 485/32 nm (32 nm bandpass filter centered at 485 nm) and 617/73 nm (73 nm bandpass filter centered at 617 nm) channels overlaid (total emission). B) 485/32 nm channel corresponding to amilFP497 emission with a lifetime colormap from 0 to 2.5 ns. C) 617/73 nm channel corresponding to the FRET-based acceptor emission with a colormap from 0.7 (similar to PE545) to 1.0 ns (similar to DOX). D) 617/73 nm channel corresponding to acceptor emission using 532 nm excitation with a colormap from 0.7 (similar to PE545) to 0.9 ns (similar to DOX). E) Overlay of B + C; the amilFP497 emission in the 485/32 nm channel and the FRET acceptor emission in the 617/73 nm channel (false red). Detailed lifetime analysis (Tables S2–S7) and phasor analysis of this data is in the Supporting Information. The scale bar represents 2 μm.

cence of the fully formed PNIPAM-*b*-amilFP497 polymersomes had its lifetime reduced from 2.98 ns (25 °C) to 1.93 ns (40 °C). This new lifetime is expected because of the close proximity of neighboring amilFP497 proteins in the polymersome morphology which leads to self-quenching of amilFP497. Importantly, in the presence of the acceptors, the formation of polymersomes was not hindered, yet some minor differences in polymersome morphology were observed (Figure 3 and Figures S19–S21).

Further, once the acceptors were encapsulated, the lifetime of the PNIPAM-*b*-amilFP497 polymersomes was reduced from 1.93 to 1.32 ns for DOX and 0.29 ns for PE545 (Table 1, Figures S20 and S21, Tables S2–S5).

We found that the PNIPAM-*b*-amilFP497 polymersomes were capable of selectively encapsulating molecules within different regions of the polymersome structure depending on their properties. The light-harvesting PE545 protein acceptor was primarily located in the membrane of the polymersomes whereas the small drug molecule (DOX) was primarily encapsulated in the aqueous core but also found in the membrane. To confirm the location of the acceptors, the samples were additionally excited using a 532 nm laser allowing no excitation of the donor, which again showed the membrane localization of the proteins, and the aqueous core and membrane locations of DOX (Figure 3D). Proteins are known to adsorb/adhere onto PNIPAM at temperatures well above the LCST[33,34] and it is therefore

Table 1: Fluorescence lifetimes based on exponential fitting of data from FLIM images (Figure 3 and Tables S2, S4, and S6) of PNIPAM-*b*-amilFP497 polymersomes encapsulating doxorubicin (DOX), the phycoerythrin 545 (PE545) protein and, the co-encapsulation of DOX + PE545.

Sample	τ_1[a]	τ_2[b]	α_1[c]	α_2[d]	χ^2[e]	E[f]
PNIPAM-*b*-amilFP497 + DOX	1.32	0.66	53	47	1.46	32%
PNIPAM-*b*-amilFP497 + PE545	0.29	1.86	83	17	2.66	85%
PNIPAM-*b*-amilFP497 + PE545 + DOX	0.30	1.86	97	3	2.60	85%

[a] Primary fluorescence lifetime. [b] Secondary fluorescence lifetime. [c] Primary lifetime pre-exponential percentage (characterizes the population of the primary lifetime species). [d] Secondary lifetime pre-exponential percentage (characterizes the population of the secondary lifetime species). [e] Fitting error in the exponential decay. [f] FRET efficiency calculated using $E = 1 - [\tau(\text{donor in the presence of acceptor})/\tau(\text{donor in the absence of acceptor})]$.

not surprising to find the light-harvesting PE545 protein in the polymersome membrane.

Interestingly, we can also co-encapsulate DOX and the PE545 protein in the same polymersome but resolve their spatial location by FLIM-FRET (Figure 3—bottom row) as the DOX and PE545 lifetimes differ quite significantly. The fluorescence lifetime maps in both the FRET (Figure 3C) and acceptor excitation—acceptor emission (Figure 3D) channels, show that the PE545 protein is localized in the membrane of the polymersomes with DOX in the interior (and presumably membrane, although the excess PE545 masks most of the DOX emission)—in line with when these molecules were loaded on their own into these polymersomes. The phasor analysis (Figure S22) and exponential tail fitting (Table S7) further confirmed this, showing the two acceptor lifetimes; about 0.4 ns from PE545 and about 1.4–1.5 from DOX. These results illustrate the power of the FLIM-FRET approach in monitoring the fate of payload mixture in a polymersome.

There is not a large difference in the diameter of our empty PNIPAM-*b*-amilFP497 polymersomes compared to those loaded with DOX, PE545 or mixtures of both (compare Figure S12 vs. Figures S23–S25) and the cloud point only increases by about 3–5 °C (Figure S9 vs. Figure S26). The PE545 and DOX protein-loaded polymersomes are about 10–20 % smaller in diameter than the empty polymersomes, suggesting that the cargo improves the packing of the PNIPAM-*b*-amilFP497 in these polymersomes.

We have shown here that the conjugation of PNIPAM with amilFP497 results in the thermoresponsive PNIPAM-*b*-amilFP497 block copolymer that forms well-defined polymersomes upon heating to 37 °C. If these polymersomes are formed in the presence of suitable fluorescent acceptors for the amilFP497 protein, the encapsulation of these acceptors can be spatially resolved using FLIM-FRET. Using this microscopy-based approach it was shown that while the water-soluble drug DOX was encapsulated in both the core and the membrane of the PNIPAM-*b*-amFP497 polymersomes, the light-harvesting PE545 protein was exclusively bound in the polymersome membranes. Importantly, we were also able to show that the PE545 protein and DOX could be co-encapsulated in these polymersomes with the resulting lifetime maps clearly revealing their different location in the polymersome membrane and core, respectively. These results demonstrate the capability of FRET-FLIM to study the encapsulation of (bio)molecular payloads by carefully designing the fluorescent properties of the polymersomes. Block copolymers based on fluorescent protein–polymer conjugates are particularly attractive in this regard as encapsulated proteins and protein–polymer bioconjugate are frequently used in functional polymersomes. We envision that this approach will be of generic use in polymersome research including in the monitoring of drug release and in the study of complex compartmentalized self-assembled structures such as vesicles-in-polymersomes.

Keywords: compartmentalization · encapsulation · FRET · polymersomes · protein modifications

How to cite: *Angew. Chem. Int. Ed.* **2015**, *54*, 5317–5322
Angew. Chem. **2015**, *127*, 5407–5412

[1] K. T. Kim, S. A. Meeuwissen, R. J. M. Nolte, J. C. M. van Hest, *Nanoscale* **2010**, *2*, 844–858.
[2] P. Tanner, P. Baumann, R. Enea, O. Onaca, C. Palivan, W. Meier, *Acc. Chem. Res.* **2011**, *44*, 1039–1049.
[3] R. P. Brinkhuis, F. P. J. T. Rutjes, J. C. M. van Hest, *Polym. Chem.* **2011**, *2*, 1449–1462.
[4] V. P. Torchilin, *Nat. Rev. Drug Discovery* **2014**, *13*, 813–827.
[5] H. Lomas, I. Canton, S. MacNeil, J. Du, S. P. Armes, A. J. Ryan, A. L. Lewis, G. Battaglia, *Adv. Mater.* **2007**, *19*, 4238–4243.
[6] E. H. C. Bromley, K. Channon, E. Moutevelis, D. N. Woolfson, *ACS Chem. Biol.* **2008**, *3*, 38–50.
[7] N. P. Kamat, J. S. Katz, D. A. Hammer, *J. Phys. Chem. Lett.* **2011**, *2*, 1612–1623.
[8] C. Martino, S.-H. Kim, L. Horsfall, A. Abbaspourrad, S. J. Rosser, J. Cooper, D. A. Weitz, *Angew. Chem. Int. Ed.* **2012**, *51*, 6416–6420; *Angew. Chem.* **2012**, *124*, 6522–6526.
[9] G. Steinberg-Yfrach, J.-L. Rigaud, E. N. Durantini, A. L. Moore, D. Gust, T. A. Moore, *Nature* **1998**, *392*, 479–482.
[10] S. F. M. van Dongen, M. Nallani, J. L. L. M. Cornelissen, R. J. M. Nolte, J. C. M. van Hest, *Chem. Eur. J.* **2009**, *15*, 1107–1114.
[11] D. Hvasanov, J. R. Peterson, P. Thordarson, *Chem. Sci.* **2013**, *4*, 3833–3838.
[12] K. Velonia, A. E. Rowan, R. J. M. Nolte, *J. Am. Chem. Soc.* **2002**, *124*, 4224–4225.
[13] S. F. M. van Dongen, H.-P. M. de Hoog, R. J. R. W. Peters, M. Nallani, R. J. M. Nolte, J. C. M. van Hest, *Chem. Rev.* **2009**, *109*, 6212–6274.
[14] X. Huang, M. Li, D. C. Green, D. S. Williams, A. J. Patil, S. Mann, *Nat. Commun.* **2013**, *4*, 2239.
[15] J. S. Lee, J. Feijen, *J. Controlled Release* **2012**, *161*, 473–483.
[16] J. Nicolas, S. Mura, D. Brambilla, N. Mackiewics, P. Couveur, *Chem. Soc. Rev.* **2013**, *42*, 1147–1235.
[17] J. W. Szostak, D. P. Bartel, P. L. Luisi, *Nature* **2001**, *409*, 387–390.
[18] P. Thordarson in *Encyclopedia of Supramolecular Chemistry* (Eds.: J. L. Atwood, J. W. Steed), Marcel Dekker, New York, **2004**, pp. 528–534.
[19] Y. Chen, J. D. Mills, A. Periasamy, *Differentiation* **2003**, *71*, 528–541.
[20] E. Zelazny, J. W. Borst, M. Muylaert, H. Bakoto, M. A. Hemminga, F. Chaumont, *Proc. Natl. Acad. Sci. USA* **2007**, *104*, 12359–12364.
[21] V. Ntziachristos, *Nat. Methods* **2010**, *7*, 603–614.
[22] C. D'Angelo, A. Denzel, A. Vogt, M. Matz, F. Oswald, A. Salih, G. Nienhaus, J. Wiedenmann, *Mar. Ecol. Prog. Ser.* **2008**, *364*, 97–106.
[23] S. Qin, Y. Geng, D. E. Discher, S. Yang, *Adv. Mater.* **2006**, *18*, 2905–2909.
[24] C. N. Lam, M. Kim, C. S. Thomas, D. Chang, G. E. Sanoja, C. U. Okwara, B. D. Olsen, *Biomacromolecules* **2014**, *15*, 1248–1258.
[25] C. S. Thomas, B. D. Olsen, *Soft Matter* **2014**, *10*, 3093–3102.
[26] M. Li, P. De, H. Li, B. S. Sumerlin, *Polym. Chem.* **2010**, *1*, 854–859.
[27] Y. Jiang, M. Liang, D. Svejkar, G. Hart-Smith, H. Lu, W. Scarano, M. H. Stenzel, *Chem. Commun.* **2014**, *50*, 6394–6397.
[28] S. H. Seo, J. Y. Chang, G. N. Tew, *Angew. Chem. Int. Ed.* **2006**, *45*, 7526–7530; *Angew. Chem.* **2006**, *118*, 7688–7692.
[29] D. M. Vriezema, J. Hoogboom, K. Velonia, K. Takazawa, P. C. M. Christianen, J. C. Maan, A. E. Rowan, R. J. M. Nolte, *Angew. Chem. Int. Ed.* **2003**, *42*, 772–776; *Angew. Chem.* **2003**, *115*, 796–800.
[30] A. B. Doust, C. N. J. Marai, S. J. Harrop, K. E. Wilk, P. M. G. Curmi, G. D. Scholes, *J. Mol. Biol.* **2004**, *344*, 135–153.
[31] E. Collini, C. Y. Wong, K. E. Wilk, P. M. G. Curmi, P. Brumer, G. D. Scholes, *Nature* **2010**, *463*, 644–647.

[32] M. A. Digman, V. R. Caiolfa, M. Zamai, E. Gratton, *Biophys. J.* **2008**, *94*, L14 – 16.
[33] D. L. Huber, R. P. Manginell, M. A. Samara, B.-I. Kim, B. C. Bunker, *Science* **2003**, *301*, 352 – 354.
[34] D. Cunliffe, C. de Las Heras Alarcón, V. Peters, J. R. Smith, C. Alexander, *Langmuir* **2003**, *19*, 2888 – 2899.

Received: December 26, 2014
Revised: February 5, 2015
Published online: March 3, 2015

